THE JOURNAL OF BIOLOGICAL CHEMISTRY
Vol. 277, No. 19, Issue of May 10, pp. 17088–17094, 2002

Printed in U.S.A.

FRS2 PTB Domain Conformation Regulates Interactions with Divergent Neurotrophic Receptors*

Received for publication, August 19, 2001, and in revised form, January 31, 2002
Published, JBC Papers in Press, February 27, 2002, DOI 10.1074/jbc.M107963200

Kelley S. Yan‡§, Miklos Kuti‡¶, Sherry Yan‡, Shiraz Mujtaba‡, Amjad Farooq‡, Mitchell P. Goldfarb‖, and Ming-Ming Zhou**

From the ‡Structural Biology Program, Department of Physiology and Biophysics, and ‖Department of Biochemistry and Molecular Biology, Mount Sinai School of Medicine, New York University, New York, New York 10029

Membrane-anchored adaptor proteins FRS2α/β (also known as SNT-1/2) mediate signaling of fibroblast growth factor receptors (FGFRs) and neurotrophin receptors (TRKs) through their N-terminal phosphotyrosine binding (PTB) domains. The FRS2 PTB domain recognizes tyrosine-phosphorylated TRKs at an NP*X*pY (where pY is phosphotyrosine) motif, whereas its constitutive association with FGFR involves a receptor juxtamembrane region lacking Tyr and Asn residues. Here we show by isothermal titration calorimetry that the FRS2α PTB domain binding to peptides derived from TRKs or FGFR is thermodynamically different. TRK binding is largely enthalpy-driven, whereas the FGFR interaction is governed by a favorable entropic contribution to the free energy of binding. Furthermore, our NMR spectral analysis suggests that disruption of an unstructured region C-terminal to the PTB domain alters local conformation and dynamics of the residues at the ligand-binding site, and that structural disruption of the β8-strand directly weakens the PTB domain association with the FGFR ligand. Together, our new findings support a molecular mechanism by which conformational dynamics of the FRS2α PTB domain dictates its association with either fibroblast growth factor or neurotrophin receptors in neuronal development.

Protein modular domains serve as molecular interfaces for interactions with proteins, nucleic acids, and phospholipids that regulate numerous cellular processes ranging from signaling of cell-surface receptors to chromosomal transcriptional regulation in the nucleus (1). The diverse functionality of these domains has been enriched through evolution such that different structural folds can perform a conserved function or a conserved fold can carry out different functions (2). Examples of the former case include the Src homology 3 and WW domains, which are structurally different but recognize related proline-rich sequences on target proteins (2–4). An example of the latter case is the phosphotyrosine binding (PTB)[1] domain (5, 6), which is structurally and functionally distinct from the SH2 domain, another conserved protein module that recognizes tyrosine-phosphorylated proteins (7, 8). The PTB domain adopts an overall fold similar to that of the pleckstrin homology domain that binds phospholipids and localizes proteins to the cell membrane (9). The prototypical PTB domains of the signaling proteins Shc and insulin receptor substrate 1 (IRS-1) preferentially bind to phosphorylated proteins containing an NP*X*pY motif, where pY is phosphotyrosine and *X* is any amino acid, with hydrophobic residues N-terminal to the sequence conferring additional specificity (10–16). Recent studies show that PTB domain-like protein modules can also bind to proteins independent of tyrosine phosphorylation or even to those lacking the canonical NP*X*Y motif. For instance, the PTB domains of X11 and Fe65 bind to an NPTY sequence in the β-amyloid precursor protein (17–19). The *Drosophila* Numb PTB domain recognizes non-NP*X*Y sequences, including GFSNMSFEDFP in the Nak Ser/Thr kinase (20, 21), and a GPY motif that was identified through screening of a tyrosine-oriented synthetic peptide library (22, 23). Furthermore, the PTB domains of the adaptor proteins Shc (10, 24) and Disabled (25) can also interact with phospholipids.

The versatility of the PTB domain superfamily is further underscored by a conserved PTB domain identified at the N terminus of the membrane-anchored adaptor proteins, FRS2α/β (fibroblast growth factor receptor substrate α/β; also known as SNT-1/2 for *suc1*-associated neurotrophic factor target) (26–29). This single FRS2 PTB domain is capable of binding different neurotrophic receptor targets in highly conserved regions that do not necessarily share any detectable sequence homology, linking receptor activation to Shp2 tyrosine phosphatase and the Ras/mitogen-activated protein kinase pathway in neuronal differentiation (30, 31). Specifically, the PTB domain of FRS2α has been shown to recognize tyrosine-phosphorylated neurotrophin receptor (TRK) at a site containing the canonical ψ*X*NP*X*pY motif, where ψ is a bulky hydrophobic residue (32, 33), and more recently to the IENKLpY sequence of the oncogenic glial cell-derived neurotrophic factor receptor RET (34, 35). Strikingly, it can also bind to the juxtamembrane region of FGFR independent of receptor phosphorylation, in a segment not even containing any Tyr or Asn residues (29, 36). Our recent solution structure of the FRS2α PTB domain in complex with a peptide derived from FGFR1 shows that the protein adopts a typical PTB domain fold consisting of a β-sandwich of two nearly perpendicular anti-parallel β-sheets

* This work was supported in part by grants from the National Institutes of Health (to M. P. G.) and the American Cancer Society (to M.-M. Z.). The costs of publication of this article were defrayed in part by the payment of page charges. This article must therefore be hereby marked "*advertisement*" in accordance with 18 U.S.C. Section 1734 solely to indicate this fact.
§ Recipient of a National Institutes of Health predoctoral fellowship.
¶ Recipient of a National Institutes of Health postdoctoral fellowship.
** To whom correspondence should be addressed: Structural Biology Program, Mount Sinai School of Medicine, 1425 Madison Ave., Box 1677, New York, NY 10029. Tel.: 212-659-8652; Fax: 212-849-2456; E-mail: zhoum@inka.mssm.edu.
[1] The abbreviations used are: PTB, phosphotyrosine binding; FGFR, fibroblast growth factor receptor; FRS, fibroblast growth factor receptor substrate; HSQC, heteronuclear single quantum coherence; ITC, isothermal titration calorimetry; IRS, insulin receptor substrate; NMR, nuclear magnetic resonance; SNT, *suc1*-associated neurotrophic factor target; pY, phosphotyrosine; TRK, neurotrophin receptor; Fmoc, *N*-(9-fluorenyl)methoxycarbonyl; IL-4R, interleukin-4 receptor.

capped by a C-terminal α-helix (38). Our structural and biochemical studies have concluded, however, that an eighth β-strand C-terminal to the α-helix unique to this particular PTB domain is critical for its association with FGFR1 but not for TRK.

In an effort to understand the mechanisms by which one protein modular domain interacts with divergent targets, we have characterized the thermodynamic properties of FRS2α PTB domain binding to FGFR1- and TRK-derived peptides by using the technique of isothermal titration calorimetry (ITC). We found that the free energy of the FRS2α PTB domain interaction with FGFR1 peptide is primarily entropy-dependent, in contrast to that of the enthalpy-dependent TRK peptide binding. Furthermore, we show by ITC and NMR analyses that truncation of residues C-terminal to the PTB domain causes structural perturbation of β8, which in turn results in alteration of local conformation and/or dynamics of the ligand-binding site residues in their binding to FGFR1 or TRK. These new results strengthen our hypothesis that local conformational perturbation involving the β8 region serves to modulate the FRS2α PTB domain association with either fibroblast growth factor or neurotrophin receptors.

EXPERIMENTAL PROCEDURES

Peptide Synthesis—Peptides used in this study were chemically synthesized at the Mount Sinai School of Medicine Protein Core Facility with Fmoc/*O*-(1H-benzotriazole-1-yl)-*N*,*N*,*N*′,*N*′-tetramethyluronium hexafluorophosphate chemistry on a MilliGen 9050 peptide synthesizer. Phosphotyrosine was incorporated using the reagent Fmoc-Tyr(PO_3H_2) with HBTU/1-hydroxy-7-azabenzotriazole activation and extended coupling times for the tyrosine and all subsequent residues. The peptides were purified by reverse phase-high performance liquid chromatography, and their compositions were confirmed by mass spectrometry.

Protein Preparation—A cDNA fragment encoding the FRS2α PTB domain (residues 11–140) was subcloned into a modified bacterial expression pET28b vector (Novagen) to produce a recombinant protein with a cleavable hexahistidine (His_6) tag at the C terminus, as described previously (38). cDNA fragments containing the desired FRS2α segments consisting of residues 11–139, 11–131, 11–122, 11–114, and 11–111 were individually cloned into the pET15b vector (Novagen) to encode N-terminally His_6-tagged recombinant proteins. Protein expression was induced with 0.3 mM isopropyl-1-thio-β-D-galactopyranoside overnight at 18 °C in transformed *Escherichia coli* BL21(DE3) cells grown to an A_{600} of 0.6 at 37 °C. After disruption of cells by freeze-thaw with lysozyme or sonication, the recombinant FRS2α proteins expressed in the soluble fraction were purified by affinity chromatography on nickel-nitrilotriacetic acid columns (Qiagen) and subsequently treated with thrombin (Sigma) to cleave off the His_6 tag. The cleaved FRS2α proteins produced with the pET28b or pET15b vector contained an additional C-terminal LVPR sequence or an N-terminal GSHM sequence, respectively.

Isothermal Titration Calorimetry Measurements—ITC experiments were performed on an Omega ITC instrument (Microcal, Northampton, MA) (39, 40). All measurements were carried out at 25 °C in 20 mM Tris-HCl buffer of pH 8.0 or 50 mM sodium phosphate buffer of pH 7.0 containing 200 mM NaCl, 1 mM EDTA, and 5 mM 2-mercaptoethanol. The synthetic peptides were dissolved in the same buffer against which the protein samples were thoroughly dialyzed and pH adjusted to match the protein solutions. The concentrations of protein and peptide solutions were 0.03–0.3 and 1–2 mM, respectively. Protein concentration was measured by the Lowry method, and peptide concentration was determined gravimetrically. The c value ($c = [\text{protein}]/K_D$, where K_D is a dissociation constant) was kept in a range of 10–200 to optimize ITC measurements (39, 41).

Each titration experiment consisted of 25 4- or 10-μl injections of a dissolved peptide into the calorimetric sample cell containing 1.34 ml of FRS2α protein solution. An initial delay of 60 s was set with an additional delay period of 250 s between each injection for the signal to return back to base line. Background reaction enthalpy was determined from injection of buffer into protein or from each peptide into buffer. In all cases, the measured enthalpies were found to be negligible compared with that of the protein and peptide binding. The background enthalpy values were subtracted from the raw titration data prior to curve fitting. Titration curves were fit to an in-built function by a non-linear least squares method with the ORIGIN software (Microcal, Northampton, MA). This function is based on binding of a ligand to a macromolecule and contains n (reaction stoichiometry), K_B (association constant), and ΔH (reaction enthalpy) as the variable parameters (39). In this fitting procedure, the values for K_B, ΔH, and n were all allowed to float. The mean value for n was found to be 1 ± 0.1. From the values of K_D ($K_D = 1/K_B$) and ΔH, the free energy (ΔG) and entropy change (ΔS) upon peptide binding to the protein can be calculated using the following relationship: $-RT\ln(1/K_D) = \Delta G = \Delta H - T\Delta S$, where R is the universal molar gas constant, and T is the absolute temperature in Kelvin (39). Errors quoted for K_D and ΔH are standard deviations from a minimum of three ITC experiments, whereas errors for $T\Delta S$ and ΔG are propagated errors.

NMR Spectroscopy—The NMR spectra of the FRS2α PTB domain were acquired on a Bruker DRX 600-MHz spectrometer at 30 °C. Uniformly ^{15}N-labeled proteins of the FRS2α PTB domain were prepared for the NMR experiments by growing bacteria that overexpress the recombinant PTB domain in M9 minimal medium containing $^{15}NH_4Cl$ as the sole nitrogen source. NMR samples contained the FRS2α PTB domain (~0.5 mM) in the free form or in complex with peptide in 100 mM sodium phosphate buffer of pH 6.5, containing 200 mM NaCl, 5 mM dithiothreitol-d_{10}, and 0.5 mM EDTA in $H_2O/^2H_2O$ (9:1). A 3-fold molar excess of a peptide was added to the protein sample before sample concentration and buffer exchange to ensure that the protein was fully saturated with the peptide. Two-dimensional ^1H-^{15}N heteronuclear single quantum coherence (HSQC) spectra were acquired with 64 and 1024 complex points in ω_1 and ω_2, respectively. NMR spectra were processed by using NMRPipe/NMRDraw (42) and analyzed with NMRView (43).

RESULTS

Binding of FGFR1 Peptide—Thermodynamic parameters of a peptide ligand binding to a protein can be obtained from ITC titration experiments (39, 40). These include the dissociation constant (K_D), reaction stoichiometry (n), enthalpy of binding (ΔH), and the Gibbs free energy change (ΔG) by a non-linear fit of the binding isotherm, as well as entropy of binding (ΔS) from a difference between the free energy change and enthalpy of binding. Given the correlation between the thermodynamic properties of an interaction and its structural characteristics, ITC data can be used to explore the different modes of receptor recognition by the FRS2α PTB domain. In an effort to examine possible protonation effects of amino acid residues on the thermodynamics of PTB domain interaction, we performed ITC measurements under two different conditions, at pH 8.0 and 7.0. The latter condition is similar to that used in the NMR study (see below).

To be consistent with the structural analysis of the FRS2α PTB domain in complex with a human FGFR1 peptide (residues 409–430) (38), we used the same FRS2α protein containing residues 11–140 in our ITC binding studies. Isothermal titration results show the PTB domain binding to the FGFR1 peptide is exothermic with 1:1 stoichiometry (Fig. 1*A*). The thermodynamic parameters determined by ITC show that the contribution to the free energy change of the FRS2α PTB domain binding to the FGFR1 peptide at pH 8.0 is dominated by a large favorable entropy change ($T\Delta S = 5.4$ kcal/mol) with a small favorable change in enthalpy ($\Delta H = -1.2$ kcal/mol) (Table I). The relative entropic and enthalpic contributions to the PTB domain/FGFR1 peptide association remain largely the same between pH 8.0 and pH 7.0.

Recognition of Tyrosine-phosphorylated NPXpY Peptides—The FRS2α PTB domain binding to tyrosine-phosphorylated NP*X*pY motif-containing TRK peptides is also exothermic, and the stoichiometry of the protein-peptide complexes is 1:1 (Fig. 1*B*). However, in contrast to the thermodynamic profile of FGFR1 interaction, the relative magnitudes of the entropy and enthalpy contribution to the free energy of the TRK peptide binding were reversed (Table I). Nevertheless, the overall free energies of association were similar between the PTB domain interactions with these two different classes of receptor ligands. The predominant contribution to TRK binding is enthal-

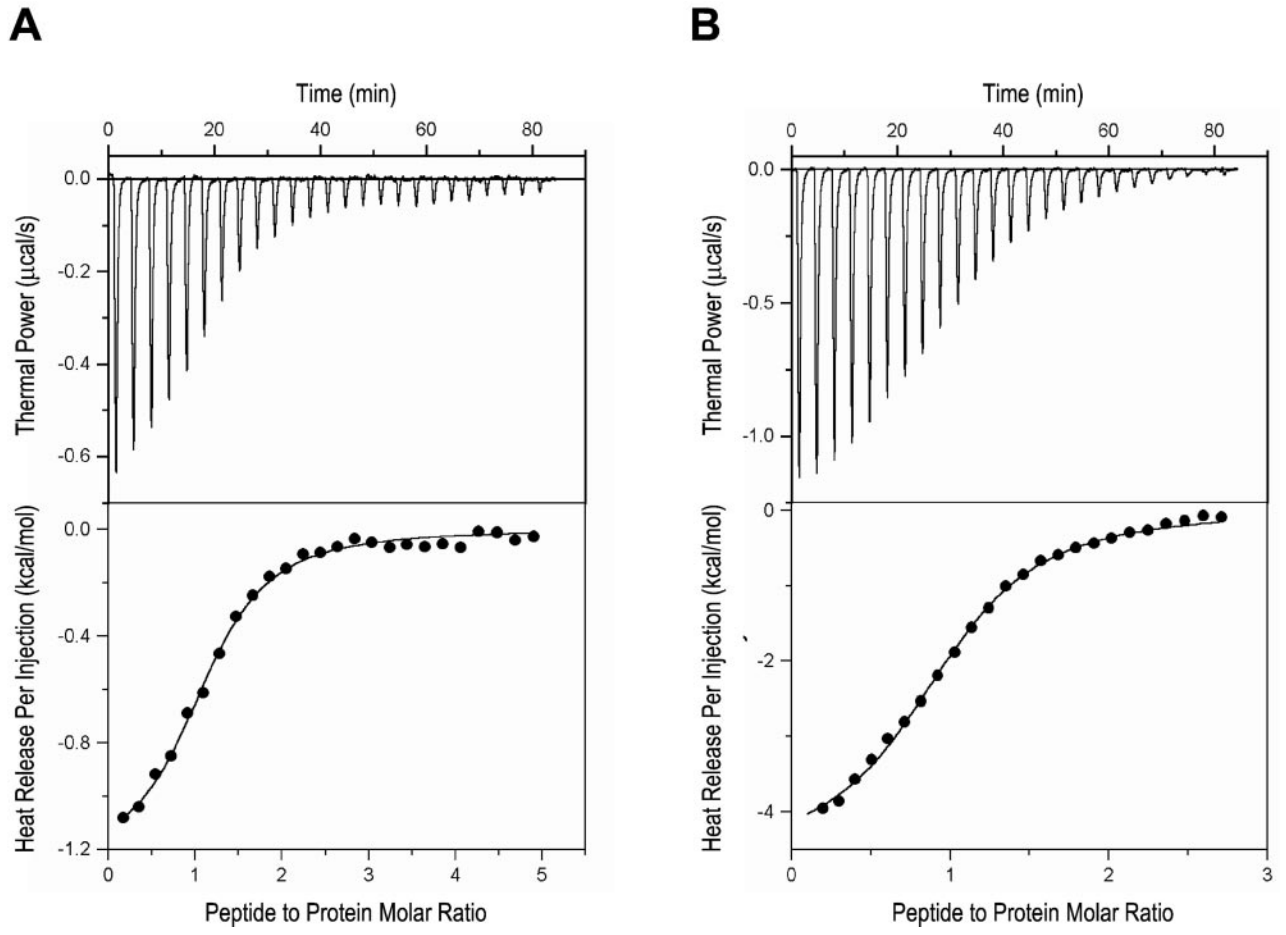

FIG. 1. **Isothermal titration calorimetry profiles of the FRS2α PTB domain (residues 11–140) binding to the FGFR1 peptide (*A*) and the tyrosine-phosphorylated TRKB peptide (*B*).** The *top panels* show the differential power time course. The total heat released in each injection is proportional to the area below the corresponding peak. The *lower panels* show a fit of the integrated areas based on peptide binding as determined by using ORIGIN software.

TABLE I
Thermodynamic parameters of the FRS2α PTB domain (residues 11–140) binding to peptides derived from different growth factor receptors, measured at pH 7.0 or 8.0 and 25 °C

Protein site	Peptide sequence	pH	K_D	ΔH	$T\Delta S$	ΔG
			μM	*kcal/mol*	*kcal/mol*	*kcal/mol*
FGFR1 (aa 409–430)	HSQMAVHKLAKSIPLRRQVTVS	8.0	13.5 ± 0.9	−1.2 ± 0.1	5.4 ± 0.1	−6.6 ± 0.04
		7.0	9.9 ± 1.0	−1.8 ± 0.2	5.0 ± 0.3	−6.8 ± 0.06
TRKB, pY61 (aa 54–65)	PVIE**NPQpY**FGIT	8.0	9.0 ± 0.5	−4.8 ± 0.2	2.1 ± 0.1	−6.9 ± 0.03
		7.0	5.2 ± 1.5	−8.0 ± 0.6	−0.8 ± 0.7	−7.2 ± 0.2
TRKA, pY490 (aa 483–494)	HIIE**NPQpY**FSDA	8.0	15.3 ± 0.5	−5.0 ± 0.2	1.5 ± 0.2	−6.5 ± 0.02
		7.0	7.7 ± 0.7	−6.5 ± 0.4	0.5 ± 0.3	−7.0 ± 0.05
TRKA (A-5), pY490	HIAE**NPQpY**FSDA	8.0	34.4 ± 5.8	−4.7 ± 0.3	1.3 ± 0.2	−6.1 ± 0.1
		7.0	23.7 ± 0.6	−5.5 ± 0.3	0.8 ± 0.3	−6.3 ± 0.02
IL-4R, pY497	LVIAG**NPApY**RS	8.0	1.0 ± 0.1	−10.3 ± 0.3	−2.1 ± 0.2	−8.2 ± 0.1
TRKA, Y490[a]	HIIE**NPQ-Y**FSDA	8.0	NA[b]	NA	NA	NA

[a] No binding was observed by the ITC measurements.
[b] Data are not available.
[c] Protein accession numbers are AAB92554 (human FRS2α), XP-049463 (human FGFR1), BAA34355 (human TRKA), AAB33110 (human TRKB), and P24394 (human IL-4R).

pic at pH 8.0 as follows: TRKA ($\Delta H = -5.0$ kcal/mol, $T\Delta S = 1.5$ kcal/mol) and TRKB ($\Delta H = -4.8$ kcal/mol, $T\Delta S = 2.1$ kcal/mol) (Table I). Similarly, at pH 7.0, the molecular recognition of the tyrosine-phosphorylated TRK peptides is also driven by a large, favorable enthalpy contribution. Notably, the affinity of the PTB domain binding to both FGFR1 and TRKA/B peptides is slightly higher at pH 7.0 than pH 8.0, resulting from a small increase of enthalpy change compensated by a reduction of entropy contribution. However, the overall magnitudes of the relative entropy and enthalpy contributions to the free energy of binding in both FGFR1 and TRK interactions remain the same between pH 7.0 and 8.0. To delineate the elements critical for the FRS2α PTB domain recognition of NP*X*pY motif-containing ligands, we performed titration studies with several related peptides. Tyrosine phosphorylation is required, as the unphosphorylated TRKA peptide exhibited no observable binding to the PTB domain by ITC (Table I). The TRKA (A-5) mutant, which contains a single amino acid substitution of Ala for Ile at phosphotyrosine 5-position, showed that binding affinity is more than 2-fold weaker than that of the wild type TRKA at both pH 8.0 and 7.0, despite a similar thermodynamic profile (Table I).

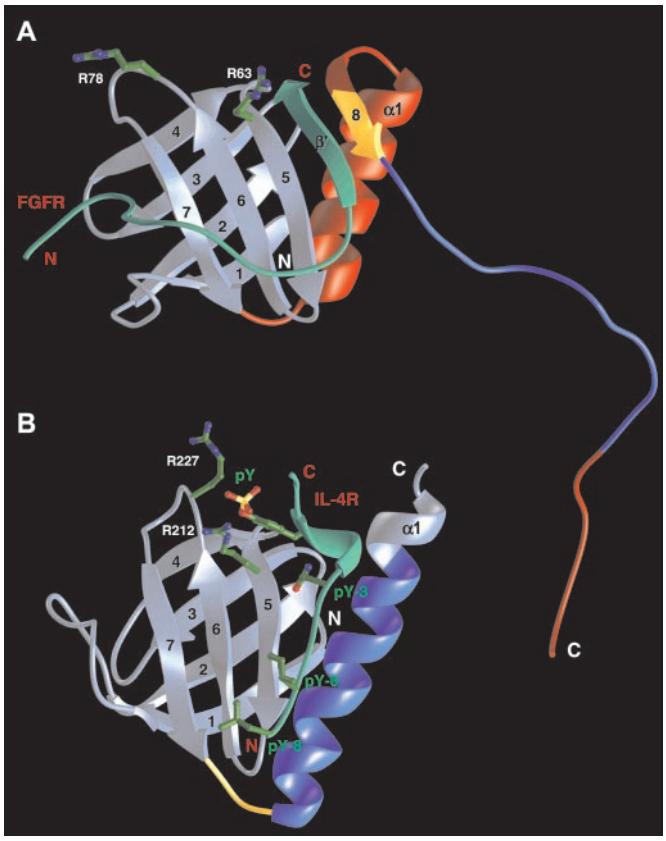

FIG. 2. **Comparison of structural and sequence homology between the PTB domains of FRS2α (*A*) and IRS-1 (*B*).** Regions of the proteins are color-coded according to sequence homology between the two PTB domains. A sequence insert corresponding to the β7/α1 loop, α1, and the N-terminal region of β8 in the FRS2α PTB domain as well as the C-terminal polyproline sequence are colored in *red*. The C-terminal portion of β8 in FRS2α and the β7/α1 loop in IRS-1 are shown in *yellow*. The region C-terminal to β8 in FRS2α and α1 (except the last turn of the helix) in IRS-1 is highlighted in *blue*. The bound peptides in both protein complexes are colored in *green*. Side chains of the two key arginine residues important for phosphotyrosine binding in each PTB domain are color-coded by atom type. Additionally, the key residues of the NPApY peptide from IL-4R important for IRS-1 PTB domain recognition are shown in *green*.

Interestingly, although the interleukin-4 receptor (IL-4R) has no known physiological function in FRS2α binding, the thermodynamic properties of its binding to the FRS2α PTB domain ($\Delta H = -10.3$ kcal/mol, $T\Delta S = -2.1$ kcal/mol) are similar to those of the IRS-1 PTB domain (Table I) (41). Although formation of new intermolecular hydrophobic and electrostatic interactions can account for the large negative enthalpy change of the complex formation, the small entropic penalty may result from the following: (i) a decrease of conformational entropy of residues that are directly involved in peptide binding and become more rigid upon complex formation; and (ii) a reduction of translational entropy of the protein and peptide upon association. These results support a notion that the two FRS2α and IRS-1 PTB domains employ an analogous mode of interaction in their recognition of NP*X*pY-containing peptides (Fig. 2, *A* and *B*).

Effect of Protein C-terminal Truncation on Receptor Peptide Binding—The structure of the FRS2α PTB domain-FGFR1 peptide complex shows that the peptide wraps around the protein to establish extensive interactions (Fig. 2*A*). The C-terminal QVTVS segment of the peptide (residues 426–430 in FGFR1) adopts an anti-parallel β-strand sandwiched between β5 and β8 of the PTB domain to form an intermolecular β-sheet. The unique β8-strand, extended from the C-terminal α-helix (α1), is not found in other known PTB domain structures. To investigate the functional role of β8 in the FRS2α PTB domain, we performed ITC studies to examine C-terminal truncation effects on FRS2α binding to FGFR1 and TRK peptides. FRS2α proteins consisting of residues 11–140, 11–139, 11–131, 11–122, 11–114, and 11–111 were used in these truncation studies (Fig. 3, *A* and *B*). ITC measurements showed that truncation of amino acid residues C-terminal to β8 did not seem to affect the PTB domain binding to FGFR1 peptide at pH 8.0 and 7.0. However, disruption of β8 conformation in the truncated FRS2α protein (residues 11–114) that lacks the last residue of β8 resulted in a marked reduction in binding affinity, *i.e.* nearly 4-fold at pH 8.0, likely through affecting the direct intermolecular interactions between β8 and β′ in the anti-parallel β-sheet (Table II). Furthermore, in the protein (residues 11–111) completely lacking β8, this decrease in affinity for FGFR1 binding was even more dramatic, although the actual K_D value could not be determined due to a significantly reduced heat change observed in the ITC titration. Likewise, binding of these two β8 truncated proteins to FGFR1 was not observed at pH 7.0 by ITC. In comparison with the full-length PTB domain, the same C-terminal β8 truncation resulted in no substantial changes in binding affinity or thermodynamic parameters in the PTB domain interaction with the TRKA peptide at pH 8.0 or to the sequence homologous TRKB peptide at pH 7.0 (Table II). It is important to note that the series of C-terminal truncations did not significantly alter the distinct thermodynamic modes of interaction of the PTB domain binding to either FGFR1 or TRK peptides. Together, these results demonstrate that β8 is indeed important for the FRS2α PTB domain binding to FGFR but not for its interaction with TRKs, and that either truncation or disruption of the β8 region greatly impairs FGFR binding. Interestingly, our findings are complemented by a recent study (37) that shows alternative splicing of FGFR1 involving its juxtamembrane region residues Val-427 and Thr-428, which directly interact with β8 of the PTB domain, affects the receptor association with FRS2α.

Effect of Protein C-terminal Truncation on Ligand-binding Site Conformation—To determine further how C-terminal truncation affects the FRS2α PTB domain function, we conducted systematic NMR spectral analysis of FRS2α binding to FGFR1 and TRK peptides by recording two-dimensional ^{1}H-^{15}N HSQC spectra with uniformly ^{15}N-labeled PTB domain, in which protein backbone amide resonances are very sensitive to changes in local chemical environment and conformation of the protein (Fig. 3, *C* and *D*). Patterns of NMR resonances of the FRS2α PTB domain bound to FGFR1 or to TRKA peptide are significantly different (Fig. 3, *C* and *D*), arguing that the PTB domain contains structural differences, at least for residues at the ligand-binding site, correlating with different receptor recognition modes.

Comparison of the HSQC spectra of the PTB domain, in complex with either FGFR1 or TRKA peptide, reveals that the overall pattern of backbone signals in each complex remained similar among the proteins with various C-terminal truncations. Notably, several protein residues in each complex (enclosed by *red dashed lines* in Fig. 3, *C* and *D*) emerged as two separate resonance peaks as more C-terminal residues were truncated. These separate resonances could not be due to the presence of both the free and ligand-bound forms because of the following: (i) the free form protein is not stable and would precipitate out of solution under these NMR conditions; and (ii) all NMR samples of the FRS2α PTB domain in complex with FGFR1 or TRKA were prepared with the peptide in molar excess, which ensures that the protein was fully saturated with ligand. Notably, although the residues that showed double

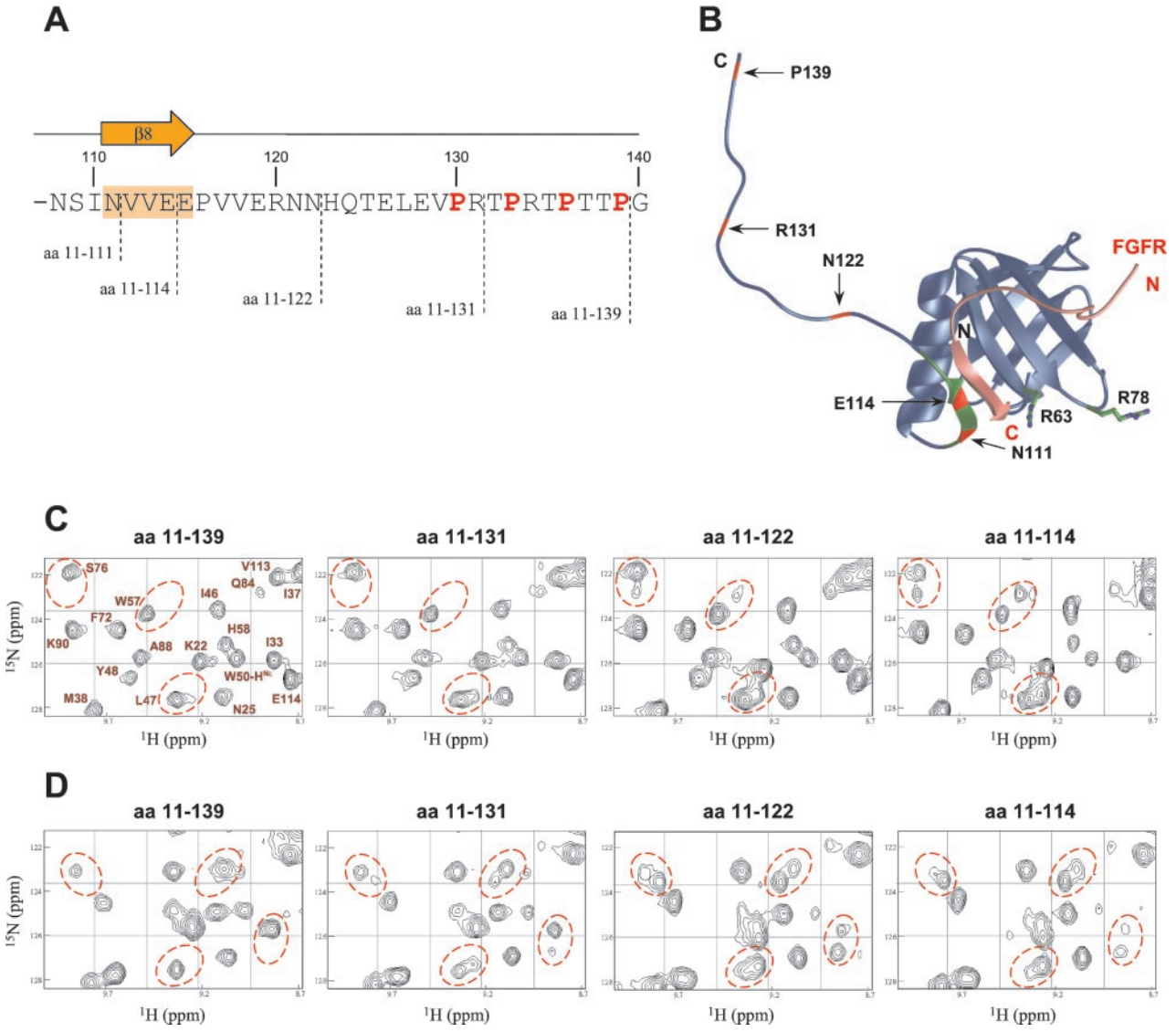

FIG. 3. **Effect of C-terminal truncation on the FRS2α PTB domain binding to FGFR and TRK peptides.** *A*, FRS2α protein sequence C-terminal to the PTB domain showing various truncations. The proline residues are highlighted in *red*. *B*, structure of the FRS2α PTB domain in complex with the FGFR peptide with *black arrows* depicting the locations of various truncations in the C-terminal segment. *C* and *D*, 2D ^{15}N HSQC spectra of the various truncated ^{15}N-labeled FRS2α PTB domain in complex with the FGFR1 (*C*) or TRKA (*D*) peptide. The amino acid residue numbers of the various FRS2α truncated proteins are indicated *above* the corresponding NMR spectra. Resonance assignments for the FRS2α PTB domain (residues 11–139) in complex with the FGFR1 peptide are shown in the HSQC spectrum. The backbone resonance peaks that show multiplicity upon truncation are enclosed in *red dashed lines*.

resonances in the TRKA-bound form remain to be assigned, those in the FGFR1-bound complex (including residues Leu-47, Trp-57, and Ser-76) are located near the ligand-binding site in the PTB domain. Therefore, these double resonance peaks in the NMR spectra may reflect differences in local conformation and/or dynamics of the protein residues at the ligand-binding site, which correspond to two distinct modes for receptor peptide recognition. These two distinct conformations of the protein are both stable and in slow exchange on the NMR time scale.

DISCUSSION

Whereas the original discovery of PTB domains is attributed to their recognition of phosphotyrosine in the context of NP*X*pY sequences, growing evidence suggests that protein modules with the PTB domain-fold have much broader ligand-binding specificities (1, 5, 6). Structural studies highlight the evolutionary changes of structural elements around the ligand-binding site on the conserved fold, which endow these protein modules with functional versatility. Thermodynamics, together with the complementary structures of protein-biological ligand complexes, can provide valuable insights into the detailed mechanisms of molecular recognition of such versatile systems (40). In this study we have characterized and demonstrated that the thermodynamics of the FRS2α PTB domain binding to two classes of unrelated neurotrophic receptor peptides are very different: FGFR1 recognition is governed by a favorable entropic contribution to the free energy of binding, whereas tyrosine-phosphorylated TRK binding is largely enthalpy-driven.

The favorable entropy change in FGFR1 binding is possibly due to structural reordering of the PTB domain, resulting from an increase in protein conformational flexibility and/or changes in solvation at the complex interface that accompanies the burial of more hydrophobic surface upon complex formation. Although the former possibility may exist, the latter is supported by the NMR structure, which reveals that the complex contains a large intermolecular interface including nearly 2025 Å^2 of buried hydrophobic surface area between the two molecules. Specifically, three bulky hydrophobic residues Val-429, Val-427, and Val-414 of the FGFR1 peptide intercalate into the

TABLE II
Thermodynamic parameters of various FRS2α PTB domain truncated proteins binding to peptides derived from FGFR1 and TRKs, measured at pH 7.0 or 8.0 and 25 °C

FRS2A PTB domain	pH	K_D	ΔH	$T\Delta S$	ΔG
		μM	*kcal/mol*	*kcal/mol*	*kcal/mol*
A. Binding to non-NPXY FGFR1 peptide					
aa 11–140 + C-terminal LVPR[a]	8.0	13.5 ± 0.9	−1.2 ± 0.1	5.4 ± 0.1	−6.6 ± 0.04
	7.0	9.9 ± 1.0	−1.8 ± 0.2	5.0 ± 0.3	−6.8 ± 0.1
aa 11–139	8.0	10.2 ± 2.3	−1.7 ± 0.4	5.1 ± 0.5	−6.8 ± 0.1
	7.0	7.2 ± 1.2	−1.3 ± 0.3	5.7 ± 0.2	−7.0 ± 0.1
aa 11–122	8.0	10.1 ± 0.6	−0.9 ± 0.1	5.9 ± 0.1	−6.8 ± 0.04
	7.0	8.8 ± 0.7	−1.3 ± 0.02	5.6 ± 0.07	−6.9 ± 0.05
aa 11–114	8.0	45.4 ± 1.4	−0.8 ± 0.1	5.1 ± 0.1	−5.9 ± 0.02
	7.0	NA	NA[b]	NA	NA
aa 11–111	8.0	NA	NA[b]	NA	NA
	7.0	NA	NA[b]	NA	NA
B. Binding to tyrosine-phosphorylated NPXpY TRK peptides[c]					
aa 11–140 + C-terminal LVPR	8.0[c]	15.3 ± 0.5	−5.0 ± 0.2	1.5 ± 0.2	−6.5 ± 0.02
	7.0[c]	5.2 ± 1.5	−8.0 ± 0.6	−0.8 ± 0.7	−7.2 ± 0.2
aa 11–139	8.0	15.5 ± 0.1	−3.9 ± 0.1	2.6 ± 0.1	−6.5 ± 0.01
	7.0	8.4 ± 0.4	−5.6 ± 0.5	1.3 ± 0.5	−6.9 ± 0.03
aa 11–122	8.0	13.4 ± 0.7	−4.5 ± 0.1	2.2 ± 0.1	−6.6 ± 0.03
	7.0	7.5 ± 1.8	−4.9 ± 0.2	2.1 ± 0.1	−7.0 ± 0.1
aa 11–114	8.0	17.6 ± 0.8	−3.6 ± 0.3	2.9 ± 0.3	−6.5 ± 0.03
	7.0	4.8 ± 0.2	−4.6 ± 0.1	2.6 ± 0.1	−7.2 ± 0.02
aa 11–111	8.0	20.7 ± 3.6	−5.7 ± 0.9	0.7 ± 0.8	−6.4 ± 0.1
	7.0	6.5 ± 0.9	−5.5 ± 0.2	1.6 ± 0.1	−7.1 ± 0.1

[a] The C-terminal LVPR sequence is part of the thrombin cleavage site engineered into the pET28b vector.
[b] Heat changes observed by ITC were too small to determine thermodynamic parameters with reliability.
[c] TRKA and TRKB peptides were used for the ITC measurements at pH 8.0 and 7.0, respectively.

hydrophobic core of the PTB domain from either side of the β-sandwich and form extensive interactions with over 13 protein residues (38). For such a highly specific complex, the enthalpy change would be expected to be much larger than that observed. However, if the PTB domain undergoes a local conformational change upon peptide binding, an associated energetic enthalpy penalty could result in an overall small ΔH of the system. Thus, these thermodynamic data suggest that the overall entropy-driven FGFR1 binding by the FRS2α PTB domain is likely due to local protein conformational restructuring to accommodate extensive hydrophobic and aromatic interactions with the peptide.

The FRS2α PTB domain binding to tyrosine-phosphorylated TRK peptides is much more exothermic than that to FGFR1, despite the fact that the latter ligand has a significantly greater number of residues that contact with the protein (as least 22 residues) than the former peptide (at most 12 residues). The large favorable enthalpy contribution associated with TRK binding could be due to intermolecular hydrophobic, electrostatic, and hydrogen bonding contacts established in the complex. While the structure of the FRS2α PTB domain in complex with a tyrosine-phosphorylated NP*X*pY-containing TRK receptor remains to be determined, several lines of evidence suggest that the mode of this molecular recognition is similar to that of the IRS-1 PTB domain binding to the IL-4R peptide (Fig. 2*B*). Supporting evidence includes the following. (i) Both PTB domains require the canonical NP*X*pY motif and its N-terminal bulky hydrophobic residues for ligand specificity (11, 38). (ii) The two key solvent-exposed arginine residues, Arg-63 and Arg-78 in FRS2α (38) and Arg-212 and Arg-227 in IRS-1 (11), essential for phosphotyrosine binding are located in structurally analogous positions in the corresponding proteins (Fig. 2). (iii) Both PTB domains bind to tyrosine-phosphorylated peptides in an overall enthalpy-driven interaction, which is exemplified by an NP*X*pY-containing peptide from IL-4R (Table I) (41). These results clearly show that both the extent of protein conformational change and the thermodynamic modes of interaction are different in FRS2α PTB domain binding to the NP*X*pY motif-containing TRK or the FGFR1 peptides.

The distinct thermodynamic modes of interaction reflect differences in the structural characteristics of FRS2α PTB domain binding to these two unrelated receptor sequences. The FRS2α and IRS-1 PTB domains share high homology in overall sequence and structural topology and recognize NP*X*pY-containing peptides in a thermodynamically similar manner. The amino acid sequences and secondary structures of the two PTB domains align extremely well but only through the β7-strand (38). Surprisingly, the FRS2α region (residues 116–136, C-terminal to the β8-strand) that exhibits high sequence homology (~45% identity) to the C-terminal α-helix in the IRS-1 PTB domain is structurally disordered (Fig. 2). The loss of helical conformation in that region of FRS2α is perhaps due to the presence of multiple proline residues that disrupts helical propensity. This divergence in the FRS2α sequence is accompanied by a new helix-forming insert (comprising residues 94–107), which is structurally analogous to the C-terminal α-helix in the IRS-1 PTB domain that blocks one side of the β-sandwich (Fig. 2, *A* and *B*). Despite their structural homology in overall three-dimensional fold, the helices are encoded by very different and divergent amino acid sequences in the two PTB domains. Moreover, residues 111–115 in FRS2α, corresponding to a sequence homologous loop between β7 and α1 in IRS-1, form β8 that interacts extensively with β′ of the FGFR1 peptide in an anti-parallel β-sheet (Fig. 2). Finally, our binding studies showed that β8 is essential for FRS2α PTB domain binding to FGFR1 but not TRK peptides (Table II) (38). The striking evolutionary change of protein sequences between two otherwise highly structurally homologous protein domains may have endowed FRS2α with greater structural plasticity, thus enabling it to recognize two very different neurotrophic receptors. The functional importance of regulating the constitutive FRS2α/FGFR association is further underscored by the recent discovery of alternative splicing of FGFR1 that directly affects the receptor interaction with the β8-strand (37).

The functional importance of the β8 and its C-terminal residues in the PTB domain is demonstrated by the observation of NMR resonance doubling of FRS2α in complex with either FGFR1 or TRK peptides upon protein C-terminal truncation. This resonance doubling suggests that truncation of the C-terminal sequence causes the protein residues at the ligand-binding site to exist in two populations with different local

chemical environment, conformation, and/or dynamics in association and dissociation with the receptor ligands. Interestingly, the resonance doubling in the TRKA peptide-bound form showed up more readily upon truncation than that of the FGFR1 peptide-complexed form. Moreover, whereas signal intensities of the double resonances in the FGFR1 complex (residues 11–114) are nearly equal, the signals corresponding to the truncation-induced conformation in the TRKA-bound form appear stronger than those of the initial conformation. These results suggest that conformational disruption of β8 of the PTB domain, induced by C-terminal truncation, perturbs the protein interaction with either FGFR1 or TRKA and particularly weakens the protein association with the FGFR1 receptor ligand. Together, our NMR analysis data strongly argue that the FRS2α PTB domain employs distinct modes of interaction involving correspondingly different ligand-binding site residues for preferential recognition of FGFR1 or TRK ligands. Perturbation of the FRS2α sequence C-terminal to the PTB domain may directly affect the structural integrity of the unique β8-strand, resulting in a conformational and thus functional switch of the protein.

Our findings have implications for a biological role of SNTs in modulating fibroblast growth factor and neurotrophin receptor signaling in neuronal survival and differentiation. The unstructured polyproline sequence C-terminal to the PTB domain could serve as a possible site of interaction with a putative signaling protein containing either an Src homology 3, WW domain, or another type of protein interaction domain. Such an interaction could disrupt and dissociate the FRS2α PTB domain from its constitutive association with FGFR, making FRS2α available for interaction with activated and tyrosine-phosphorylated TRKs in developing neurons. Our new thermodynamic and NMR structural results demonstrate how a conserved protein modular domain has evolved to acquire the structural plasticity necessary to recognize two very different ligands by altering a short region in the protein sequence, and how this unique structural capability enables this domain to regulate distinct biological processes in neuronal development.

Acknowledgments—We thank Christophe Dhalluin, Olga Plotnikova, and Lei Zeng for technical advice on protein sample preparation and NMR experiments.

REFERENCES

1. Pawson, T., and Nash, P. (2000) *Genes Dev.* **14,** 1027–1047
2. Pawson, T., and Scott, J. D. (1997) *Nature* **278,** 2075–2080
3. Mayer, B. J. (2001) *J. Cell Sci.* **114,** 1253–1263
4. Sudol, M., Sliwa, K., and Russo, T. (2001) *FEBS Lett.* **490,** 190–195
5. Yan, K. S., Kuti, M., and Zhou, M.-M. (2002) *FEBS Lett.,* **513,** 67–70
6. Forman-Kay, J. D., and Pawson, T. (1999) *Curr. Opin. Struct. Biol.* **9,** 690–695
7. Kuriyan, J., and Cowburn, D. (1993) *Curr. Opin. Struct. Biol.* **3,** 828–837
8. Pawson, T. (1995) *Nature* **373,** 573–580
9. Lemmon, M. A., Ferguson, K. M., and Schlessinger, J. (1996) *Cell* **85,** 621–624
10. Zhou, M.-M., Ravichandran, K. S., Olejniczak, E. T., Petros, A. P., Meadows, R. P., Sattler, M., Harlan, J. E., Wade, W., Burakoff, S. J., and Fesik, S. W. (1995) *Nature* **378,** 584–592
11. Zhou, M.-M., Huang, B., Olejniczak, E. T., Meadows, R. P., Shuker, S. B., Miyazak, M., Trüb, T., Shoelson, S. E., and Fesik, S. W. (1996) *Nat. Struct. Biol.* **3,** 388–393
12. Eck, M. J., Dhe-pagnon, S., Trüb, T., Nolte, R., and Shoelson, S. E. (1996) *Cell* **85,** 695–705
13. Blaikie, P., Immanuel, D., Wu, J., Li, N., Yajnik, V., and Margolis, B. (1994) *J. Biol. Chem.* **269,** 32031–32034
14. Kavanaugh, W. M., and Williams, L. T. (1994) *Science* **266,** 1862–1865
15. Kavanaugh, W. M., Turck, C. W., and Williams, L. T. (1995) *Science* **268,** 1177–1179
16. Gustafson, T. A., He, W., Craparo, A., Schaub, C. D., and O'Meill, T. J. (1995) *Mol. Cell. Biol.* **15,** 2500–2508
17. Borg, J.-P., Ooi, J., Levy, E., and Margolis, B. (1996) *Mol. Cell. Biol.* **16,** 6229–6241
18. Zambrano, N., Buxbaum, J. D., Minopoli, G., Fiore, F., Candia, P. D., Renzis, S. D., Faraonio, R., Sabo, S., Cheetham, J., Sudol, M., and Russo, T. (1997) *J. Biol. Chem.* **272,** 6399–6409
19. Zhang, Z., Lee, C.-H., Mandiyan, V., Borg, J.-P., Margolis, B., Schlessinger, J., and Kuriyan, J. (1997) *EMBO J.* **16,** 6141–6150
20. Chien, C. T., Wang, S., Rothenberg, M., Jan, L. Y., and Jan, Y. N. (1998) *Mol. Cell. Biol.* **18,** 598–607
21. Zwahlen, C., Li, S.-C., Kay, L. E., Pawson, T., and Forman-Kay, J. D. (2000) *EMBO J.* **19,** 1505–1515
22. Li, S.-C., Songyang, Z., Vincent, S. J. F., Zwahlen, C., Wiley, S., Cantley, L., Kay, L. E., Forman-Kay, J., and Pawson, T. (1997) *Proc. Natl. Acad. Sci. U. S. A.* **94,** 7204–7209
23. Li, S.-C., Zwahlen, C., Vincent, S. J., McGlade, C. J., Kay, L. E., Pawson, T., and Forman-Kay, J. D. (1998) *Nat. Struct. Biol.* **5,** 1075–1083
24. Ravichandran, K. S., Zhou, M.-M., Pratt, J. C., Harlan, J. E., Walk, S., Fesik, S. W., and Burakoff, S. J. (1997) *Mol. Cell. Biol.* **17,** 5540–5549
25. Howell, B. W., Kanier, L. M., Frank, R., Gertler, F. B., and Cooper, J. A. (1999) *Mol. Cell. Biol.* **19,** 5179–5188
26. Wang, J.-K., Xu, H., Li, H.-C., and Goldfarb, M. (1996) *Oncogene* **13,** 721–729
27. Kouhara, H., Hadari, Y. R., Spivak-Kroizman, T., Schilling, J., Bar-Sagi, D., Lax, I., and Schlessinger, J. (1997) *Cell* **89,** 693–702
28. Hadari, Y. R., Kouhara, H., Lax, I., and Schlessinger, J. (1998) *Mol. Cell. Biol.* **18,** 3966–3973
29. Ong, S. H., Guy, G. R., Hadari, Y. R., Laks, S., Gotoh, N., Schlessinger, J., and Lax, I. (2000) *Mol. Cell. Biol.* **20,** 979–989
30. Xu, H., and Goldfarb, M. (2001) *J. Biol. Chem.* **276,** 13049–13056
31. Ip, N. Y., Boulton, T. G., Li, Y., Verdi, J. M., Birren, S. J., Anderson, D. J., and Yancopoulos, G. D. (1994) *Neuron* **13,** 443–455
32. Meakin, S. O., MacDonald, J. I. S., Gryz, E. A., Kubu, C. J., and Verdi, J. M. (1999) *J. Biol. Chem.* **274,** 9861–9870
33. Peng, X., Greene, L. A., Kaplan, D. R., and Stephens, R. M. (1995) *Neuron* **15,** 395–406
34. Melillo, R. M., Santoro, M., Ong, S.-H., Billaud, M., Fusco, A., Hardari, Y. R., Schlessinger, J., and Lax, I. (2001) *Mol. Cell. Biol.* **21,** 4177–4187
35. Kurokawa, K., Iwashita, T., Murakami, H., Hayashi, H., Kawai, K., and Takahashi, M. (2001) *Oncogene* **20,** 1929–1938
36. Xu, H., Lee, K. W., and Goldfarb, M. (1998) *J. Biol. Chem.* **273,** 17987–17990
37. Burgar, H. R., Burns, H. D., Elsden, J. L., Lalioti, M. D., and Heath, J. K. (2002) *J. Biol. Chem.* **277,** 4018–4023
38. Dhalluin, C., Yan, K. S., Plotnikova, O., Lee, K. W., Zeng, L., Kuti, K., Mujtaba, S., Goldfarb, M. P., and Zhou, M.-M. (2000) *Mol. Cell* **6,** 921–929
39. Wiseman, T., Williston, S., Brandts, J. F., and Lin, L. N. (1989) *Anal. Biochem.* **179,** 131–137
40. Jelesarov, I., and Bosshard, H. R. (1999) *J. Mol. Recognit.* **12,** 3–18
41. Farooq, A., Plotnikova, O., Zeng, L., and Zhou, M.-M. (1999) *J. Biol. Chem.* **274,** 6114–6121
42. Delaglio, F., Grzesiek, S., Vuister, G. W., Zhu, G., Pfeifer, J., and Bax, A. (1995) *J. Biomol. NMR* **6,** 277–293
43. Johnson, B. A., and Blevins, R. A. (1994) *J. Biomol. NMR* **4,** 603–614